Quantum Theoretical Evidence for Two Distinct Hydrogen-Bonding Networks and for an Ising Chain Model of the Antiferroelectric Transition in Squaric Acid

J. Palomar[†] and N. S. Dalal*[,‡]

Departamento de Química Física Aplicada, Universidad Autónoma de Madrid, Madrid, Spain, and Department of Chemistry, Florida State University, Tallahassee, Florida 32306-4390

Received: September 12, 2001; In Final Form: November 7, 2001

The electronic structure of squaric acid ($H_2C_4O_4$, SQA) has been investigated by density functional techniques at the B3LYP/6-31G** level to understand the mechanism of the paraelectric-to-antiferroelectric phase transition in the compound at 373 K. A nonsymmetrical structure without a C_4 axis has been used for the first time. Monomer, dimer, and pentamer models of the SQA system were used to assess the possible differences between the two intersecting O−H···O chains. Despite the use of a small cluster size, we felt that the noted differences in the energetics and related characteristics of the two chains in the crystal lattice are realistic. This result suggests different proton dynamics along the chains and thus argues against the generally accepted 2-D phase-transition behavior. The calculations also help explain the literature discrepancies involving earlier ^{13}C NMR and diffraction data. They support a model in which the phase transition is triggered by thermally induced disorder of the H atoms in the more π-resonant O···H−O bonds, which in turn leads to the 3-D ordering of the two mutually perpendicular Ising-type chains.

1. Introduction

This investigation reports on a quantum theoretical study of the O−H···O bonding in squaric acid, $H_2C_4O_4$, henceforth SQA (structure shown in Figure 1). This study was undertaken because although SQA has been studied extensively experimentally[1−17] as well as theoretically[18−21] (since the discovery of its paraelectric-to-antiferroelectric transition at $T_c = 373$ K[1]), the atomistic details of the mechanism underlying the phase transition and the accompanying dielectric and other anomalies around the T_c are still not fully understood. We focused on the O−H···O bonding because it is well accepted that either an order−disorder or tunneling motion of the O−H···O protons must play a pivotal role in the mechanism because deuteration raises the T_c from 373 to 543 K.[1] In particular, following the earlier X-ray[2,3] and neutron diffraction[4,5] studies, recent neutron and Raman scattering measurements[6−9] have indicated that the earlier accepted 2-D model of the SQA structure and its phase transition might not be accurate and that the two O−H···O chains might in fact have different ordering dynamics. Some support for this conclusion has been provided by the recent very high-resolution ^{13}C solid-state NMR studies in the vicinity of its phase transition.[10−12] These NMR studies detected four distinct ^{13}C peaks in the isotropic (magic angle spinning) spectra of SQA in its low-temperature, antiferroelectric phase. This new result was in contrast to some earlier NMR reports[13−17] wherein the number of peaks had been reported to be only two. Although this discrepancy could be ascribed to the low resolution in the earlier NMR studies,[13−16] the question of whether the two O−H···O chains are energetically different remained. In this regard, it may be noted that in its crystalline lattice, SQA consists of planar molecular layers where each C_4O_4 group is connected to its neighboring four units by strong O−H···O hydrogen bonds.[1−7] At room temperature, the H atoms are asymmetrically distributed in the O···H−O bonds, each SQA molecule presenting an ordered structure with two vicinal and two distal protons and clearly localized single and double bonds. The polar SQA molecules are aligned along the same direction in the molecular plane, thus describing a 2-D ferroelectric structure. Neighboring layers, however, have their electric polarization in opposite directions, and this arrangement results is a 3-D antiferroelectric structure, the sheets being bonded by weak van der Waals interactions. Above T_c (373 K), the SQA structure changes from the monoclinic (C_{1h}) to tetragonal (C_{4h}) molecular symmetry, with the C_4O_4 unit at the 4-fold axis and the proton equally distributed on two equivalent sites in the hydrogen bond. The individual layers, therefore, carry no spontaneous polarization, and the crystal becomes paraelectric. Although these studies imply that the SQA lattice is a model 2-D system, the aforementioned neutron data of Semmingsen et al.[8] pointed to a 1-D model, with each O−H···O chain being somewhat independent but with significant interaction between the two O−H···O chains. To our knowledge, these discrepancies have not yet been resolved.

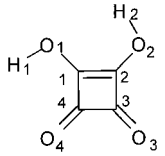

Figure 1. Squaric Acid Skeleton.

The present study was undertaken with the view of obtaining theoretical evidence for the possible difference in the two O−H···O networks in the SQA crystal, to obtain a detailed theoretical understanding of the temperature dependence of the recent ^{13}C NMR results,[10−12] and to obtain new clues about the phase-transition mechanism. To this end, we have used the well-established density functional method by employing several molecular clusters of SQA to reproduce the crystal environment.

* Corresponding author. E-mail: dalal@chem.fsu.edu.
[†] Universidad Autónoma de Madrid.
[‡] Florida State University.

10.1021/jp013486u CCC: $22.00
Published on Web 04/10/2002

SCHEME 1

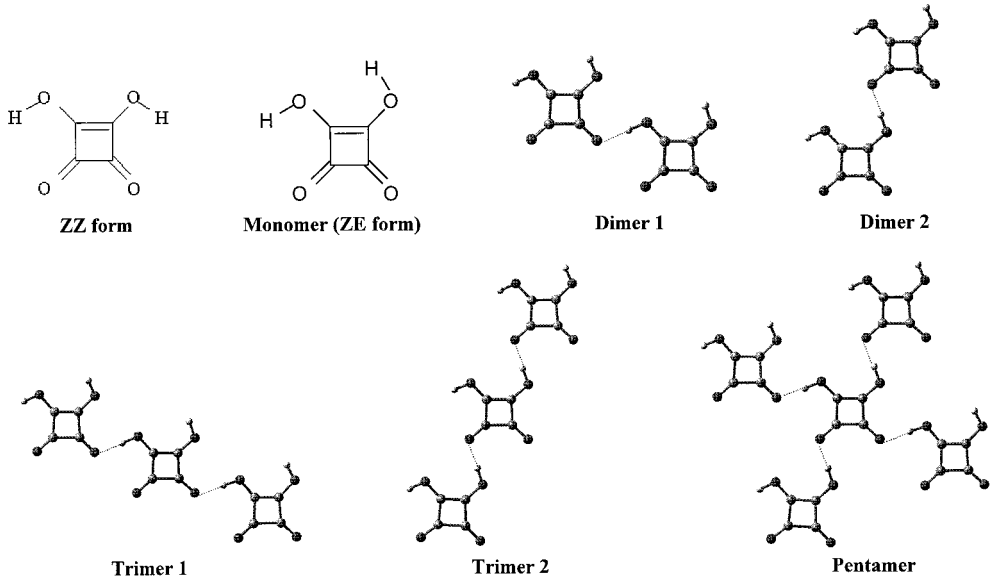

An important aspect of this work is that we have used the nonsymmetrical unit cell without the presence of a C_4 axis. Also, we focus on detecting any possible differences in the two O−H···O chains, which are thought to yield realistic results despite a small cluster size because of the possible cancellation of the truncation effects. Because of our computational limitations, the largest model we consider is the pentamer (see Scheme 1) (i.e., an approximation of the hydrogen-bonding network). Scheme 1 presents two hydrogen bonds in each different trimer chain, which can be considered a reasonable approximation because it represents 87% of the cooperative effects as has been demonstrated by Dannenberg and co-workers[22,23] for the case of the RAHB-type hydrogen bonds. The hybrid B3LYP method in combination with the medium basis set 6-31G** is used as an acceptable compromise between the accuracy of the calculations and their computational cost.[24] We found that even with this compromise the calculations yield significantly new insight into the nature of bonding and phase transition in SQA,and may have general implications for other hydrogen-bonded systems.

2. Computational Details

All the molecular geometries and energies have been calculated using the B3LYP method[25,26] in conjunction with a 6-31G** basis set. To avoid the interaction effects between the surrounding SQA units, the 2-D SQA molecular clusters were optimized at the B3LYP/6-31G** level, fixing the hydrogen bond angles given by neutron diffraction data at 15 K but leaving the rest of the coordinates free. Additionally, the pentamer model (Scheme 1) was fully optimized by ONIOM[27,28] (B3LYP/6-31G**: PM3) methodology as the high-level layer with eight additional SQA units linked to the free pentamer functional groups as the lower-level layer. Both methods used to construct the pentamer model provide very similar results. The isotropic NMR nuclear shieldings (^{13}C σ_{iso}) were calculated at the B3LYP/6-31G** level using the GIAO[29,30] method. The conversion to chemical shifts (^{13}C δ_{iso}) was done using the experimental−theoretical linear correlation obtained from the current results of SQA.

All computations were performed with the aid of the Gaussian 98 program.[31]

3. Results and Discussion

3.1. Molecular Structure and Hydrogen Bonding. The isolated SQA molecule has been studied recently by MP2 and B3LYP methods in combination with medium and large basis sets.[18−21] The results obtained showed the most stable conformation for the ZZ isomer among the three possible planar conformers (see Scheme 1). Consistently, the ZZ species has been shown to be responsible for the infrared spectra of SQA isolated in low-temperature Ar and N_2.[18] The theoretical analysis described the ZZ form of SQA clearly shows aromatic character because C═O, C═C, C−O, and C−C groups showed partially missed double and single bond character by the effect of the resonance along the HO−C═C−C═O chains (Scheme 2).[18] However, the ZZ conformer of SQA in a matrix is different from that found in the crystalline state at room temperature, where the intermolecular hydrogen bonds stabilize the ZE form (see Scheme 1). As expected, the calculated geometries for the isolated ZE structure showed strong variations from those obtained by X-ray and neutron diffraction measurements.[18,19] These structural differences should be clearly attributed to the hydrogen bond effects and the expected larger resonance (Scheme 2) in the solid state. Therefore, the first goal of our present work was to develop an adequate computational model for analyzing the electronic structure of SQA in the crystal. Six SQA models (monomer, dimers, trimers, and pentamer in Scheme 1) were used in the quantum chemical calculations of this study. Table 1 summarizes the bond distances of the B3LYP/6-31G** geometries for the molecular clusters considered.

SCHEME 2

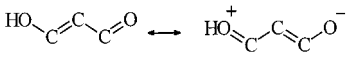

The monomer model represents the gas-phase ZE structure of SQA. We find that the results obtained at the B3LYP/6-31G** level (Table 1) are almost identical to those obtained using higher computational levels.[18] The optimized ZE form presents C_{1h} symmetry and C═C and C═O distances that are significantly elongated whereas the C−C and C−O distances are shortened relative to those in the parent compounds cyclobutandione (C═O = 1.198 Å; C−C = 1.583 Å) and cyclobutenediol (C−O = 1.369 Å; C═C = 1.343 Å). These bond character changes are similar to those previously found for the ZZ form, being attributed to the contribution of the resonance to the H−O−C═C−C═O structures in the SQA molecule. However, in contrast to the ZZ species, the optimized

TABLE 1: Bond Distances (Å) of SQA from the B3LYP/6-31G Geometries and from Neutron Diffraction Measurements**

	monomer	dimer 1	dimer 2	trimer 1	trimer 2	pentamer	exp, 15 K[8]	exp, RT[8]
C_1-O_1	1.333	1.323	1.332	1.312	1.333	1.311	1.290	1.289
C_2-O_2	1.327	1.329	1.316	1.330	1.302	1.307	1.286	1.287
$C_3=O_3$	1.203	1.209	1.202	1.219	1.202	1.219	1.228	1.227
$C_4=O_4$	1.208	1.206	1.216	1.204	1.227	1.222	1.232	1.230
$C_1=C_2$	1.377	1.308	1.383	1.386	1.391	1.401	1.413	1.414
C_3-C_4	1.563	1.557	1.555	1.550	1.546	1.531	1.497	1.500
C_2-C_3	1.500	1.486	1.502	1.471	1.505	1.477	1.461	1.461
C_1-C_4	1.484	1.492	1.472	1.500	1.459	1.477	1.464	1.464
O_1-H_1	0.971	0.980	0.971	0.997	0.971	0.994	1.038	1.030
O_2-H_2	0.970	0.970	0.979	0.970	0.995	0.992	1.043	1.037
$O_1\cdots O_{3'}$		2.710		2.662		2.686	2.533	2.553
$O_2\cdots O_{4'}$			2.726		2.678	2.712	2.544	2.554
$H_1\cdots O_{3'}$		1.725		1.673		1.700	1.496	1.524
$H_2\cdots O_{4'}$			1.744		1.689	1.725	1.501	1.517
E_{HB}[a]		9.2	10.1	21.2	22.6	39.7		
μ[a]	5.7	13.9	13.6	23.1	22.5	38.8		

[a] Calculated hydrogen bond energies (E_{HB}, kcal/mol) and dipole moments (μ, D) of the molecular models studied at the B3LYP/6-31G** level.

ZE form shows two slightly different H−O−C═C−C═O systems. As we can see in Scheme 1, the ZE molecule presents two different weak intramolecular hydrogen bonds. It should be noted that the $H_2-O_2-C_2=C_1-C_4=O_4$ chain contributes to these hydrogen bonds through $C_4=O_4$ as an acceptor and O_2H_2 as a donor whereas the hydroxyl O_1-H_1 group is a donor and an acceptor simultaneously. This fact should cause stronger polarization in the $H_2-O_2-C_2=C_1-C_4=O_4$ system and thus larger π-electron delocalization along this chain. Consequently, the calculated ZE geometry shows shorter C−O and C−C bonds and a longer C═O bond for this chain (see Table 1). Therefore, the calculations suggest different resonant character in the two H−O−C═C−C═O systems of the asymmetric ZE conformations in the crystal.

The dimer models contain two ZE molecules linked by one intermolecular hydrogen bond. Because two slightly distinct intermolecular hydrogen bonds are formed by O_1-H_1 and O_2-H_2 groups, which are respectively located anti and syn to the $C_1=C_2$ double bond, two different dimers are analyzed in this study (Scheme 1). To describe the global hydrogen bond effect, we average the B3LYP/6-31G** bond distances of the two SQA molecules included in each dimer (Table 1). As expected, the main finding is that the hydrogen bond causes a significant lengthening of the OH bond that is involved. Moreover, an elongation of the calculated C═C and C═O double bonds and a shortening of the C−C and C−O single bonds are observed in the hydrogen-bonded chain compared to those of the isolated molecule. These results are clearly attributed to the increasing contribution of the resonance to the H−O−C═C−C═O structure by the hydrogen bond interaction. Therefore, we find computational evidence of an important cooperative phenomenon between the hydrogen bonding and the electronic delocalization on SQA.[32,33] On the other hand, we observe that the hydrogen-bonded $H_2-O_2-C_2=C_1-C_4=O_4$ chain in dimer 2 is a more highly conjugated double bond system than the hydrogen-bonded $H_1-O_1-C_1=C_2-C_3=O_3$ structure in dimer 1. Moreover, distinct hydrogen bond geometry is obtained for dimer 1 and dimer 2 clusters (Table 1). Therefore, our calculations clearly show different hydrogen-bonded systems along the two diagonal directions in SQA. To analyze such differences, we have calculated an approximation of the hydrogen bond energy for SQA as $\Delta E = E_{HB}$ in Eq. (1a) of Scheme 3. We thus find a slightly greater hydrogen bond strength in $O_{4'}\cdots H_2-O_2$ (E_{HB} (dimer 2) = 10.1 kcal/mol) than in $O_{3'}\cdots H_1-O_1$ (E_{HB}(dimer 1) = 9.2 kcal/mol). Because it is well-known that the π resonance strongly stabilizes this type of hydrogen-bonded system,[32,33] this finding is consistent with a more π-resonant system along the $H_2-O_2-C_2=C_1-C_4=O_4$ coordinate. In contrast, a shorter hydrogen bond structure is found for $O_{3'}\cdots H_1-O_1$ (see O···H, O···O, and O−H distances in Table 1), indicating a more effective electrostatic attraction between the donor and acceptor groups in this hydrogen bond. As a consequence, current results suggest that two different H−O−C═C−C═O chains remain in the hydrogen-bonded SQA compound.

SCHEME 3

2 × SQA (Monomer) ↔ Dimer	$\Delta E = E_{HB}$ (Dimer)	Eq. (1a)
3× SQA (Monomer) ↔ Trimer	$\Delta E' = E_{HB}$ (Trimer)	Eq. (1b)
5× SQA (Monomer) ↔ Pentamer	$\Delta E'' = E_{HB}$ (Pentamer)	Eq. (1c)

The next model examined is the trimer structure, where two SQA units are hydrogen bonded to a central SQA molecule in such a way that the latter structure participates in two identical hydrogen bonds (see Scheme 1). The B3LYP/6-31G** geometry for the central molecule of the two possible trimer models (trimers 1 and 2 in Scheme 1) is summarized in Table 1. One significant result is that a much greater influence of the cooperative resonance hydrogen-bonding phenomena is observed for the doubly linked H−O−C═C−C═O chain in the trimer structures. Thus, the SQA units are closer in the trimer than in the dimer structures (see O−H, O···O, and H···O distances in Table 1), suggesting a stronger attraction between OH and C═O groups. In addition, the global energy of the two hydrogen bonds in the trimers (E_{HB} (trimer1)/E_{HB} (trimer 2) = 21.2/22.6 kcal/mol by eq 1b of Scheme 3) is slightly greater than twice the hydrogen bond energy obtained from the dimers, which indicates higher resonance stabilization by the formation of the second hydrogen bond in the H−O−C═C−C═O chain. Mainly, greater differences are observed from the doubly hydrogen-bonded π-resonant system of trimer 2 to that of trimer 1.

The final cluster constructed at the B3LYP/6-31G** level consists of a pentamer structure where the central SQA molecule is involved in four intermolecular hydrogen bonds with the neighboring SQA units (Scheme 1). Therefore, the pentamer model should represent a reasonable first description of the hydrogen-bonding network around an SQA molecule in the crystal lattice. If one compares the B3LYP/6-31G** molecular structure of the pentamer with those of the monomer, dimers, and trimers, it seems clear that the pentamer correctly reproduces the neutron diffraction data (Table 1). Thus, the B3LYP/6-31G** bond-distance order for the central SQA molecule of

the pentamer exhibits almost full agreement with the experimental order but with C_4O_4 bond distances systematically differing by 0.01−0.02 Å. Significantly, the $C_1-C_2-O_2$ and $C_2-O_2-H_2$ angles are theoretically predicted to be 1.3° and 1.2° larger than the $C_4-C_1-O_1$ and $C_1-O_1-H_1$ angles, respectively, in good agreement with the experimental results that were noted to be the main structural difference between the two hydrogen bonds in SQA.[8] However, we find stronger deviations concerning the hydrogen bond distances that are probably due to the limitation of the pentamer model in reproducing the cooperative effect in the crystal chains. Thus, calculations predict that the $O_2\cdots O_{4'}$ and $H_2\cdots O_{4'}$ bonds are longer than the corresponding distances in the $O_1-H_1\cdots O_{3'}$ system, which agrees with neutron diffraction data at 15 K but with significant deviations of 0.1−0.2 Å. Strangely, the experimental O_2-H_2 bond is also longer than O_1-H_1, which seems to contradict the rest of the hydrogen bond distances. Some light can be shed on these misleading data if one analyzes the available hydrogen bond structure at different temperatures.[8] Thus, at room temperature (RT), a greater difference between both hydroxyl groups is observed (see Table 1), but now the $H_2\cdots O_{4'}$ distance is shorter than the $H_1\cdots O_{3'}$ distance and the O···O distances are almost identical. In fact, the RT structural data are consistent with a shorter $O_{4'}\cdots H_2-O_2$ hydrogen bond, in contrast with the evidence at 15 K. On the other hand, the reported data on the O_2-H_2 distance showed a significantly greater spread (0.073 Å) than did the data on the O_1-H_1 distance (0.012 Å).[2,4,8] These findings may be related to the greater disorder found for the H_2 proton. It is our view that the experimental − calculated differences shown in Table 1 may be attributed to the different temperature dependence of the two hydrogen bond geometries in the SQA crystal.

The analysis of the B3LYP/6-31G** results for the pentamer provides evidence for the highest overall conjugation in the strained ring of an SQA molecule when it is linked by four hydrogen bonds. However, single and double bonds are still recognizable in the optimized pentamer structure, in good agreement with the fully ordered crystal of SQA at low temperatures. The pentamer results clearly lead to the following conclusion: Two clearly different diagonal coordinates, which are directed along the two different doubly hydrogen-bonded resonant chains of the compound, are distinguishable in the structure. Thus, a more effective resonance is established in the $H_2-O_2-C_2=C_1-C_4=O_4$ system at the expense of that in the opposite $H_1-O_1-C_1=C_2-C_3=O_3$ chain. On the contrary, a shorter $O_{3'}\cdots H_1-O_1$ bond is observed in the central molecule of the system. These results suggest the complex electrostatic−covalent nature of the hydrogen bond systems in SQA, as one might expect. As a global effect, the pentamer is stabilized by 39.7 kcal/mol by the four hydrogen bond interactions and shows slightly longer hydrogen bonds relative to those of the smaller trimer clusters, providing evidence of some competitive effect between the two diagonal resonances. However, it should be mentioned that the bond distances of the hydrogen-bonded C−O and C=O groups are close to the corresponding distances in the trimer models, thus indicating the near-global independence between both H−O−C=C−C=O chains. In fact, a similar conclusion is reached from the structural analysis of the dimer and trimer clusters. Thus, in these structures, although the C_3-C_4 bond is shortened by the effect of the conjugation in the ring, the non-hydrogen-bonded O−H, C−O, and C=O groups remain almost unaffected by the hydrogen bond effect (see Table 1). In other words, the differently conjugated H−O−C=C−C=C−C=O chains in SQA seem to be virtually independent of each other.

TABLE 2: Comparisons of Calculated ^{13}C NMR Chemical Shifts[a] from the Theoretical SQA Models with the Experimental Data Obtained from High-Resolution Solid-State NMR Spectroscopy[10]

	monomer	dimer 1	dimer 2	trimer 1	trimer 2	pentamer	exp
C1	184.2	188.9	182.4	192.3	180.4	187.1	187.0
C2	186.9	184.6	189.3	184.1	192.4	187.8	187.7
C3	187.6	192.0	186.0	196.4	184.2	192.9	193.9
C4	193.1	188.4	197.4	186.7	201.3	195.0	194.3

[a] Experimental−theoretical linear correlation: $^{13}C\ \delta_{iso} = 200 - 0.95 \times {}^{13}C\ \sigma_{iso}$ (Sd = 0.9 ppm, $R = 0.983$)

Finally, it is interesting to mention the anomalous increase of the calculated dipole moment with the size of the system, revealing the higher polarity of SQA by the hydrogen bond effect: monomer (5.7 D), dimer 1/2 (13.9/13.6 D), trimer 1/2 (23.1/22.5 D) and pentamer (38.8 D),

3.2. ^{13}C NMR Analysis. The calculation of the NMR parameters for the isolated ZE form of SQA by the GIAO method at the B3LYP/6-31G** level provides four slightly different ^{13}C chemical shifts ($^{13}C\ \delta_{iso}$, see Table 2). These results provide additional evidence of the distinctly different electronic structure of each carbon fragment of the asymmetric ring of SQA. It should be noted that lower ^{13}C shielding in the couple $C_2(-O_2H_2)$ and $C_4(=O_4)$ than in $C_1(-O_1H_1)$ and $C_3(=O_3)$ is related to the lower electron density around the C_2 and C_4 atoms of the more π-conjugated chain $H_2-O_2-C_2=C_1-C_4=O_4$.

With the aim of understanding the dependence of NMR parameters on the hydrogen-bonding environment in SQA, we calculated the ^{13}C chemical shifts for the different molecular clusters discussed above (i.e., the dimer, trimer, and pentamer models; see Table 2). From the comparison between the predicted NMR data, it is evident that the $^{13}C\ \delta$ values of hydroxyl carbons and carbonyl carbons increase because of the presence of the hydrogen bonds in the molecule. This finding can be simply attributed to the stronger π-electron delocalization along both hydrogen-bonded H−O−C=C−C=O systems. On the other hand, those carbon atoms of C=O and C−OH groups that are not involved in the hydrogen bonds of the dimer and trimer structures exhibit higher chemical shielding compared to those of the isolated SQA species (see Table 2) as a result of the decreased π conjugation in the attached H−O−C=C−C=O system. In the case of the pentamer cluster, both phenomena happen simultaneously, and they partially cancel each other. As a global effect, the hydrogen bonds on the central SQA molecule in the pentamer cause a slight increase in the ^{13}C chemical shift in all the carbon atoms of the ring with respect to the monomer model (Table 2) according to a general increase of the aromaticity in the full hydrogen-bonded structure. In this respect, we observe that the presence of four hydrogen bonds diminishes the differences between the $^{13}C\ \delta_{iso}$ values of the two hydroxyl carbons of the SQA molecule, suggesting a more equitable electron distribution around these atoms in the pentamer than in the isolated molecule. A similar conclusion is arrived at from the $^{13}C\ \delta$ values of the carbonyl carbons. In this respect, the pentamer model includes a fairly complete hydrogen-bonding network of SQA in quantum chemical calculations. Therefore, it is the only cluster considered that can be reasonably used to analyze the ^{13}C NMR spectra of crystalline SQA. Recently, our group showed[10−12] that the high-resolution ^{13}C NMR spectra of single SQA crystals exhibited four different isotropic chemical shifts (see Table 2) corresponding to the four C atoms in SQA. These signals were

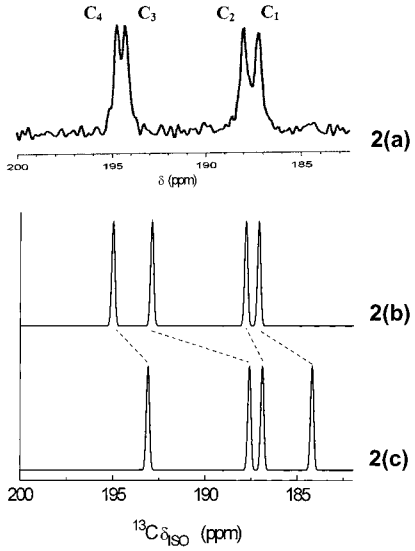

Figure 2. (a) Typical solid-state ^{13}C CP/MAS NMR spectra of an SQA single crystal.[10] (b) Theoretically calculated ^{13}C NMR spectrum for SQA using the pentamer model. (c) Theoretically calculated ^{13}C NMR spectrum for an isolated molecule of SQA by the GIAO-B3LYP/6-31G** method.

assigned on the basis of bond distance considerations. As can be seen in Figure 2, our calculated NMR data for the pentamer excellently reproduce the experimental results, showing full agreement with the published conclusions (Table 2) and corroborating the hypothesis of four different carbon atoms in the SQA crystal.[10] The NMR signals at 187.0 and 193.9 ppm are assigned, respectively, to the C_1 and C_3 atoms whereas the peaks at 187.7 and 194.3 ppm are consistently attributed to the couple C_2 and C_4. Therefore, computational results predict that the ^{13}C signals of the C_2, C_4 couple are shifted to higher ppm values relative to those of C_1, C_3 according to the greater electron delocalization detected on the C_2 and C_4 fragments. Thus, C_2 and C_4 atoms possess higher ^{13}C chemical shifts even when the computational model provides longer hydrogen bond distances for the $O_{4'}\cdots H_2-O_2$ system. In fact, these results have already been found for the monomer, dimer, and trimer structures of SQA. Therefore, we inferred that the lower shielding on the C_2 and C_4 atoms is due to the more effective electronic migration along the $H_2-O_2-C_2=C_1-C_4=O_4$ chain rather than the proton position inside the O···O bond.

3.3. Phase Transition. As alluded to in the Introduction, both neutron diffraction and recent NMR data point to the increasing amount of disorder in the entire SQA structure with increasing temperature as well as distinctly different behavior for the protons of the two different hydrogen bonds.[8,10,12] The present calculations support the fact that the H_2 proton should show significantly more disorder than the H_1 proton on the basis of the predominant fluctuations in the π-electron system along the $H_2-O_2-C_2=C_1-C_4=O_4$ chain. Taking into account the practical independence of the two O−H···O chains, these findings suggest that the primary cause of the disorder in SQA with increasing temperature is a proton excitation at the H_2 site, which results in a pseudorotation of the molecule by +90° around the axis that is perpendicular to the SQA plane by the interchange of single and double bonds within the π-conjugated system.[8] As this proton flipping interchanges the roles of the two protons, one can infer that the (correlated) dynamics of H_2 and H_1, which clearly must play a key role in the phase transition, would be confined to only one double-minimum potential along the pseudorotational coordinate because each of the two reaction pathways is characterized by one of the two distinct hydrogen

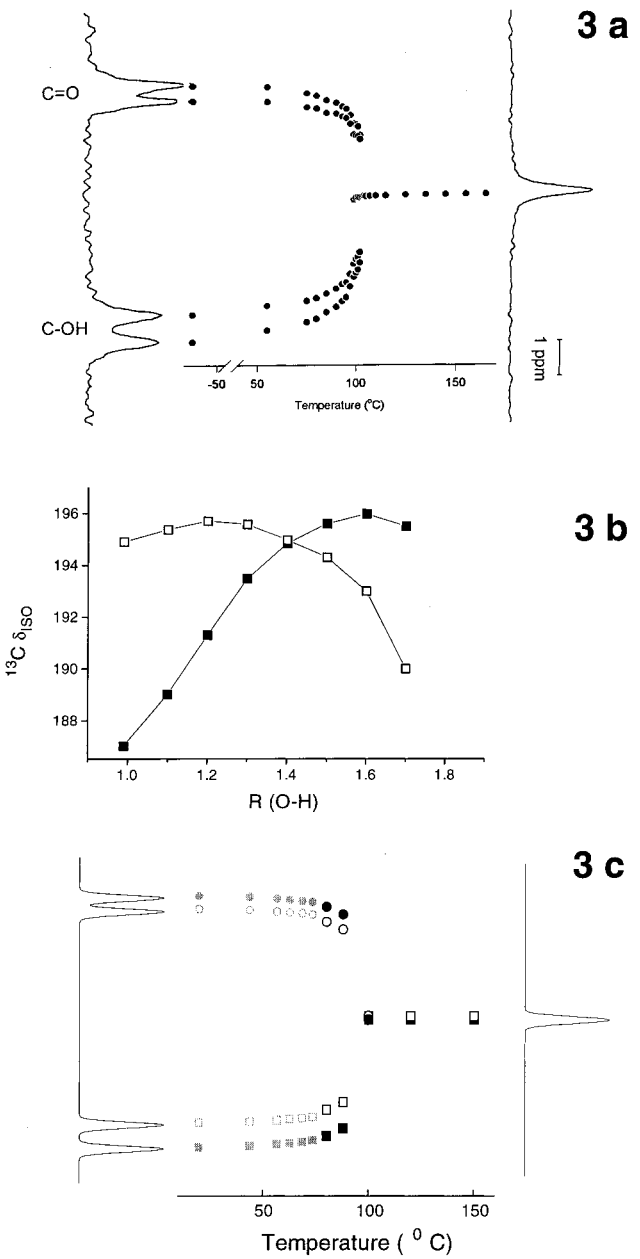

Figure 3. (a) Temperature dependence of ^{13}C CP/MAS NMR spectra of SQA obtained by solid-state high-resolution NMR measurements.[10] (b) Proton position dependence of the ^{13}C chemical shifts of C_2 (■) and C_4 (□) calculated at the B3LYP/6-31G** level using the double-proton-transfer curve in the pentamer model. (c) Temperature dependence of the ^{13}C chemical shifts of SQA obtained as an average of the C_1/C_4 and C_2/C_3 experimental values.[36]

bonds in the system. Thus, although the proton disorder should originate in the $O_2-H_2\cdots O_{4'}$ chain, the dynamics of the hydrogen atoms in both of the chains in SQA should be strongly coupled.

Our earlier NMR studies had suggested that one could perhaps employ the position of the H atom as an order parameter of the phase transition.[10] To examine this conjecture quantitatively, we calculated the ^{13}C NMR signals as a function of the proton position in the pentamer model. As mentioned earlier, on approaching T_c, the hydroxyl and carbonyl ^{13}C NMR doublets move closer together and merge into one peak at the phase transition (see Figure 3a).[10] The computationally predicted behavior in the chemical shifts of the C_2 and C_4 atoms of the central molecule of the pentamer when the proton is moved along the $O_{4'}\cdots H_2-O_2$ coordinate is shown in Figure 3b. Clearly,

the predicted ^{13}C NMR signals of the carbonyl and hydroxyl groups show a different dependence on the O−H distance than on the temperature. Thus, the chemical shift of the C−OH fragment greatly increases when the proton is moved away toward the intermediate zone of the proton transfer, but the ^{13}C peak of the C═O group does not decrease, as expected, but increases in this first region of the curve. This finding is clearly explained by the stronger influence of the electronic redistribution in the H−O−C═C−C═O chain by the opposite hydroxyl change rather than by the effect of the proton approximation. In the second region of the transfer ($R_{OH} > 1.4$ Å) when the proton is moving close to the carbonylic oxygen, the chemical shift of this group diminishes drastically toward values that are close to those of a C−OH fragment, but the ^{13}C signal of the hydroxyl group behaves like that of a C═O group in the first region of the transfer, revealing the practically interchanged character of the functional groups during the process. As result, our computational results invalidate an earlier model of a single-minimum potential in the high-temperature structure of SQA with the proton placed in the middle of the O···O distance.[34] In fact, we have observed that any slight lengthening of the OH bond (from the hydrogen bond effect or a proton-transfer process) increases the ^{13}C chemical shifts of both the carbonyl and the hydroxyl carbons attached to the chain. Therefore, we believe that the temperature dependence of the ^{13}C chemical shifts (Figure 3a) results from a time averaging of the partially disordered SQA structure. Considering the pseudorotation mechanism proposed for the proton motion, we note that the environments of C_2 and C_4 after the proton flip of H_2 should correspond closely to those of the ordered C_3 and C_1 sites, respectively. In addition, the initial C_1 and C_3 gradually obtain C_4 and C_2 character, respectively, through such +90°pseudorotation. Under this hypothesis, the temperature-dependent values of the chemical shifts of the carbon atoms result from statistical contributions from a carbonyl and a hydroxyl group with different hydrogen bond environments. At high temperatures (above T_c), the process of proton flipping should happen simultaneously in both directions of the double-well potential (i.e., along the two diagonal coordinates), and, as a consequence, the electronic distribution of each carbon fragment of the system should result from the contributions of the four possible environments. This model may explain the decreases in the splittings of the two main doublets of SQA when the temperature approaches T_c from $T < T_c$, merging in one peak at higher temperatures close to T_c. In fact, the experimental ^{13}C chemical shift average of the crossed couples C_1/C_4 and C_2/C_3 are practically overlapped: 190.65 and 190.8 ppm. In Figure 3c, we present the ^{13}C chemical shift of SQA obtained by applying the refined site occupancies for the hydrogen atoms at different temperatures[8] (and also the occupation probabilities of the double-well potential given by Samuelsen et al.[35]) as a fractional function of the carbonyl and hydroxyl contributions to the ^{13}C chemical shifts.[36] The evident similarity between this representation and that of the experimental behavior of the ^{13}C NMR data at increasing temperature (Figure 3a) is consistent with the model proposed.

Finally, the interaction between layers has been invoked to account for the 4-fold disorder transition.[8] Thus, as the temperature increases, the interlayer separation increases. On the basis of the model proposed here, the in-plane dynamics of the proton provide diagonal chains with reversed polarity, thereby decreasing the attractive interactions between the layers. The dynamics of both H_1 and H_2 should be favored in this situation and consequently should favor the 4-fold disorder in the system. Then, the experimental evidence of the low-temperature symmetry retained locally above T_c, and vice versa, may be associated with the fact that the phase transition in a specific layer seems to occur at the expense of the transition in the surrounding layers.

4. Summary and Conclusions

We have presented a detailed density functional analysis of SQA using several 2-D molecular clusters in combination with the hybrid density functional method B3LYP and a 6-31G** basis set. As a result, we have obtained the first computational evidence of the close connection between hydrogen bonding and π conjugation in the SQA system. Significantly, our calculations suggest that the two O···H−O chains in SQA might be energetically different, supporting the conclusion obtained from neutron diffraction data. Thus, the larger disorder in the $H_2-O_2-C_2=C_1-C_4=O_4$ system is consistent with the greater π conjugation in this diagonal coordinate shown by the current density functional study. The ^{13}C chemical shifts are theoretically described and are shown to be a sensitive probe of the electronic distribution in this type of system and support the suggestion that the two (diagonal) O···H−O chains are chemically different. These results suggest a new model of the phase transition in SQA: the mechanism involves the order−disorder behavior of protons in two distinct and practically independent hydrogen-bonded HO−C═C−C═O chains, in line with the neutron data.[8] Thermally induced flipping of the H_2 proton initiates the phase transition, resulting in a pseudorotation of the molecule by 90° and interchanging the roles of the H_2 and H_1 protons. The pseudorotational process of the trapezoidal form implies a drastic change of the electronic structure of the system, which provokes a displacement in the center of mass of the molecule. Consecutive pseudorotations along the diagonal coordinates lead to the superposition of the four different orientations of the trapezoidal molecule, resulting in a disordered structure above T_c. The change of the dipole moment orientation by the proton flipping possibly contributes to the increase of the interlayer separation, thereby favoring the transition process.

We note, however, that the present study uses only a finite cluster size, thus only the relative difference between the chains is reliable. Additional calculations involving a much larger cluster size are needed to put the proposed model on firmer footing.

Acknowledgment. This research was supported in part by a grant from the National Science Foundation and Florida State University. We acknowledge Centro de Computación Científica of Universidad Autónoma de Madrid for the computer time.

References and Notes

(1) Semmingsen, D. *Solid State Commun.* **1974**, *15*, 1369.
(2) Semmingsen, D. *Acta Chem. Scand.* **1973**, *27*, 3961.
(3) Semmingsen, D. *Tetrahedron Lett.* **1973**, *11*, 807.
(4) Semmingsen, D.; Hollander, F. J.; Koetzele, T. F. *J. Chem. Phys.* **1977**, *66*, 4405.
(5) Hollander, F. J.; Semmingsen, D.; Koetzele, T. F. *J. Chem. Phys.* **1977**, *67*, 4825.
(6) Sammuelsen, E. J.; Semmingsen, D. *J. Phys. Chem. Solids* **1977**, *38*, 1275.
(7) Sammuelsen, E. J.; Fjaer, E.; Semmingsen, D. *J. Phys. C: Solid State Phys.* **1979**, *12*, 2007.
(8) Semmingsen, D.; Tun, Z.; Nelmes, R. J.; McMullan, R. K.; Koetsle, T. F. *Z. Kristallogr.* **1995**, *210*, 934.
(9) Ehrhardt, K. D.; Buchenau, U.; Sammuelsen, E. J.; Maier, H. D. *Phys. Rev. B: Condens. Matter* **1984**, *29*, 996.
(10) Klymachyov, A. N.; Dalal, N. S. *Z.Phys. B: Condens. Matter* **1997**, *104*, 651. *Solid State Nucl. Magn. Reson.* **1997**, *9*, 85. *Ferroelectrics* **1998**, *206−207*, 103.

(11) Fu, R.; Klymachyov, A. N.; Bodenhausen, G.; Dalal, N. S. *J. Phys. Chem. B* **1998**, *102*, 8732.
(12) Dalal, N. S.; Klymachyov, A. N.; Bussmann-Holder, A. *Phys. Rev. Lett.* **1998**, *81*, 5924.
(13) Blinc, R.; Zeks, B. *Phys. Rev. Lett.* **1977**, *38*, 92.
(14) Mehring, M.; Suwelack, D. *Phys. Rev. Lett.* **1979**, *42*, 317.
(15) Mehring, M.; Becker, J. D. *Phys. Rev. Lett.* **1981**, *47*, 366.
(16) Kuhn, W.; Maier, H. D.; Petersson, J. *Solid State Commun.* **1979**, *32*, 249.
(17) Seliger, J.; Zager, V.; Blinc, R. *J. Magn. Reson.* **1984**, *58*, 349.
(18) Rostkowska, H.; Nowak, M. J.; Lapinski, L.; Smith, D.; Adamowicz, L. *Spectrochim. Acta, Part A* **1997**, *53*, 959.
(19) Zhou, L.; Zhang, Y.; Wu, L.; Li, J. *J. Mol. Struct.* **2000**, *497*, 137.
(20) Spassova, M.; Kolev, T.; Kanev, I.; Jacquemin, D.; Champagne, B. *J. Mol. Struct.* **2000**, *528*, 151.
(21) Rovira, C.; Novoa, J.; Ballone, P. *J. Chem. Phys*. **2001**, *115*, 6406.
(22) Turi, L.; Dannenberg, J. J. *J. Phys. Chem.* **1992**, *96*, 5819.
(23) Dannenbeg, J. J.; Haskamp, L.; Masunov, J. *J. Phys. Chem*. **1999**, *103*, 7083.
(24) Barone, V.; Adamo, C. *Int. J. Quantum Chem.* **1997**, *61*, 429.
(25) Becke, A. D. *J. Chem. Phys.* **1993**, *98*, 5648.
(26) Lee, C.; Yang, W.; Parr, R. G. *Phys. Rev. B: Solid State* **1988**, *37*, 785.
(27) Svensson, M.; Humbel, S.; Froese, R. D. J.; Matsubara, T.; Sieber, S.; Morokuma, K. *J. Phys. Chem.* **1996**, *100*, 19 357.
(28) Humbel, S.; Sieber, S.; Morokuma, K. *J. Chem. Phys.* **1996**, *105*, 1959.
(29) Wolinski, K.; Hilton, J. F.; Pulay, P. *J. Am. Chem. Soc*. **1990**, *112*, 8251.
(30) Dietchfield, R. *Mol. Phys.* **1974**, *27*, 789.
(31) Frisch, M. J.; Trucks, G. W.; Schlegel, H. B.; Scuseria, G. E.; Robb, M. A.; Cheeseman, J. R.; Zakrzewski, V. G.; Montgomery, J. A., Jr.; Stratmann, R. E.; Burant, J. C.; Dapprich, S.; Millam, J. M.; Daniels, A. D.; Kudin, K. N.; Strain, M. C.; Farkas, O.; Tomasi, J.; Barone, V.; Cossi, M.; Cammi, R.; Mennucci, B.; Pomelli, C.; Adamo, C.; Clifford, S.; Ochterski, J.; Petersson, G. A.; Ayala, P. Y.; Cui, Q.; Morokuma, K.; Malick, D. K.; Rabuck, A. D.; Raghavachari, K.; Foresman, J. B.; Cioslowski, J.; Ortiz, J. V.; Stefanov, B. B.; Liu, G.; Liashenko, A.; Piskorz, P.; Komaromi, I.; Gomperts, R.; Martin, R. L.; Fox, D. J.; Keith, T.; Al-Laham, M. A.; Peng, C. Y.; Nanayakkara, A.; Gonzalez, C.; Challacombe, M.; Gill, P. M. W.; Johnson, B. G.; Chen, W.; Wong, M. W.; Andres, J. L.; Head-Gordon, M.; Replogle, E. S.; Pople, J. A. *Gaussian 98*; Gaussian, Inc.: Pittsburgh, PA, 1998.
(32) Bertolasi, V.; Gilli, P.; Ferretti, V.; Gilli, G. *Chem.—Eur. J.* **1996**, *2*, 925.
(33) Gilli, P.; Bertolasi, V.; Ferreti, V.; Gilli, G. *J. Am. Chem. Soc.* **1994**, *116*, 909.
(34) Pumpernik, D.; Mendas, I.; Bvorstnik, B.; Azman, A. *J. Phys. Chem. Solids* **1979**, *40*, 463.
(35) Sammuelsen, E. J.; Buchenau, U.; Dieter, M.; Ehrhardt, K.; Fjaer, E.; Grimm, H. *Phys. Scr*. **1982**, *25*, 685.
(36) Predicted ^{13}C chemical shifts for the couples C_1/C_4 and C_2/C_3 obtained as $^{13}C\ \delta_{iso}(C_1/C_4) = X_{H1}(187.0/194.3) + (1 - X_{H1})(194.3/187.0)$ and $^{13}C\ \delta_{iso}(C_2/C_3) = X_{H2}(187.7/194.3) + (1 - X_{H2})(194.3/187.7)$ where X_{H1} and X_{H2} are the experimental proton occupancies at 80, 88, 106, and 122 °C (ref 8) or the double-well potential occupancies below T_c from ref 35.